JOURNAL OF NANO- AND ELECTRONIC PHYSICS
Vol. **10** No 6, 06016(4pp) (2018)
ЖУРНАЛ НАНО- ТА ЕЛЕКТРОННОЇ ФІЗИКИ
Том **10** № 6, 06016(4cc) (2018)

The Structural-Phase State and Diffusion Process in Film Structures Based on Co and Ru

I.V. Cheshko[1,*], A.M. Lohvynov[1], A.I. Saltykova[2], S.I. Protsenko[1]

[1] *Sumy State University, 2, Rimsky-Korsakov Str., 40007 Sumy, Ukraine*
[2] *Sumy State Pedagogical University named after A.S. Makarenko, 87, Romens'ka Str., 40002 Sumy, Ukraine*

(Received 15 August 2018; revised manuscript received 04 December 2018; published online 18 December 2018)

Investigation results of crystalline structure, phase composition and diffusion processes in film systems based on Co and Ru in the thickness range 5÷60 nm before and after annealing to temperature 600 K are represented. It was shown that the film system Co / Ru / S and Co / Ru / Co / S consist of a phase hcp-Co and hcp-Ru. Film systems consisting of Ru layers before and after annealing have a nanodispersed crystalline texture. The average size of crystallites samples before annealing does not exceed 3÷5 nm, after annealing the maximum average size was 16 nm for samples with layer thicknesses 60 nm. The results of the study of the diffusion process of two-layer film systems Co / Ru / in different thickness ranges showed that before and after annealing the relative individuality of separate layers is preserved since the calculated values of thermal diffusion effective coefficients for relatively thin and thick films lie in the range from 0.1 to $1.1 \cdot 10^{-19}$ m²/ sec.

Keywords: Thin film, Synthetic antiferromagnetic layer, Crystal structure, Phase composition, Diffusion, Secondary ion mass spectrometry.

DOI: 10.21272/jnep.10(6).06016

PACS numbers: 05.70. – a, 61.72.Mm, 61.72.Lk, 62.20.F –, 64.10. + h, 64.60.My, 68.35.Md, 83.10. – y

1. INTRODUCTION

A necessary condition for obtaining a simple metal spin-valve-type device structures according scheme «magnetic working layer 1 / non-magnetic layer / magnetic working layer 2» for the needs of modern functional solid-state and flexible electronics is to ensure the stability of the interface between magnetism and nonmagnetic layers. Traditional application of thin nonmagnetic layers Cu [1], Ag [2] or Au [3] for separation of magnetic Co, Fe or their alloys working layers is accompanied by problems arising from the intensive condensation-stimulated and thermal diffusion between these layers, the destruction of interfaces and the formation of disordered solid solutions. As a result, the magnetic layers lose the ability to be reversed individually and the entire structure ceases to function as a spin valve. This phenomenon was investigated by the authors of works [1, 3-5] on the example of metal pseudo-spin-valve structures.

Solving this problem by the authors of the works [6, 7] application of additional buffer thin layers was considered. But the result is a reduction in the effective performance of such structures. Authors [8] offer a technique for additional thermal treatment of individual layers of these metals in the process of receiving spin-valves although this only achieves a temporary beneficial effect. An alternative may be to use a layer material from other metals, such as a Gd or Dy layer as shown in the works [9, 10]. According to the data [11, 12] reliable layer separation Co or NiFeCuMo possible by using thin layers with Ru thickness from 0.2 ÷ 3 nm. Such structures were proposed to be used to form synthetic antiferromagnetic layers for creating spin-valves because they are realized strong indirect exchange coupling and perpendicular magnetic anisotropy.

But the application of such a combination is complicated by the complexity of obtaining homogeneous crystalline Ru layers and Limited data on the structural and phase state of two- and multi-layer film systems based on Ru and Co. The purpose of this study was to establish the optimal conditions for obtaining three and multilayer film systems based on Co and Ru with temperature-stable interfaces between separate layers for the formation of simple spin-valve type functional metal structures.

2. EXPERIMENTAL TECHNIQUE

In the study received film system in a single-layer films Ru / S (S – substrate) and Co / S, two-layer Ru / Co / S and three-layer systems Co / Ru / Co / S and multi-layers [Ru (2) / Co (2)]$_5$ / S (in brackets the thickness is specified in nm). The thickness of individual layers was 5÷60 nm and controlled by the quartz resonator method in the process of samples forming. Layers metals condense on the substrate by electron-beam gun in a vacuum (pressure of the residual atmosphere 10^{-5} Pa). The substrates were carbon flexible thin films of a thickness 20 nm (for the electron microscopic studies by transmission electron microscopy device ПЕМ-125К) and silicon single crystal plate with silicon dioxide layer (Si/SiO_2 (500 nm)) 1 × 1 sm format (for the study of diffusion processes between separate layers by the method of secondary ion mass spectrometry (SIMS) by the device MS-7201M). To study the influence of heat treatment on the structural characteristics of the formed samples, annealing was carried out to a temperature T_a = 600 K with constant heating and cooling speed 4÷5 K / min. in vacuum (the pressure of the residual atmosphere 10^{-6} Pa). Value T_a = 300 K meets the samples without annealing.

*cheshko.iryna@gmail.com

3. EXPERIMENTAL RESULTS

The results of the study of the crystalline structure of Co, Ru, two- and multilayer film systems are presented as micro-images on Fig. 1. The crystalline structure of single-layer Ru films essentially depends on the thickness. Before annealing in the whole range of film thicknesses the average size of crystallites is of order 2÷3 nm. After annealing, the average crystallite size is significantly increased for samples thicker than 30 nm (Fig. 1 b, b′). For Co films before and after annealing can observe homogeneous hexagonal structure with average crystallite size 5÷7 nm (Fig. 1 a, a′). Only for relatively thin Co layers with thickness near 5 nm samples have a nanodispersed structure.

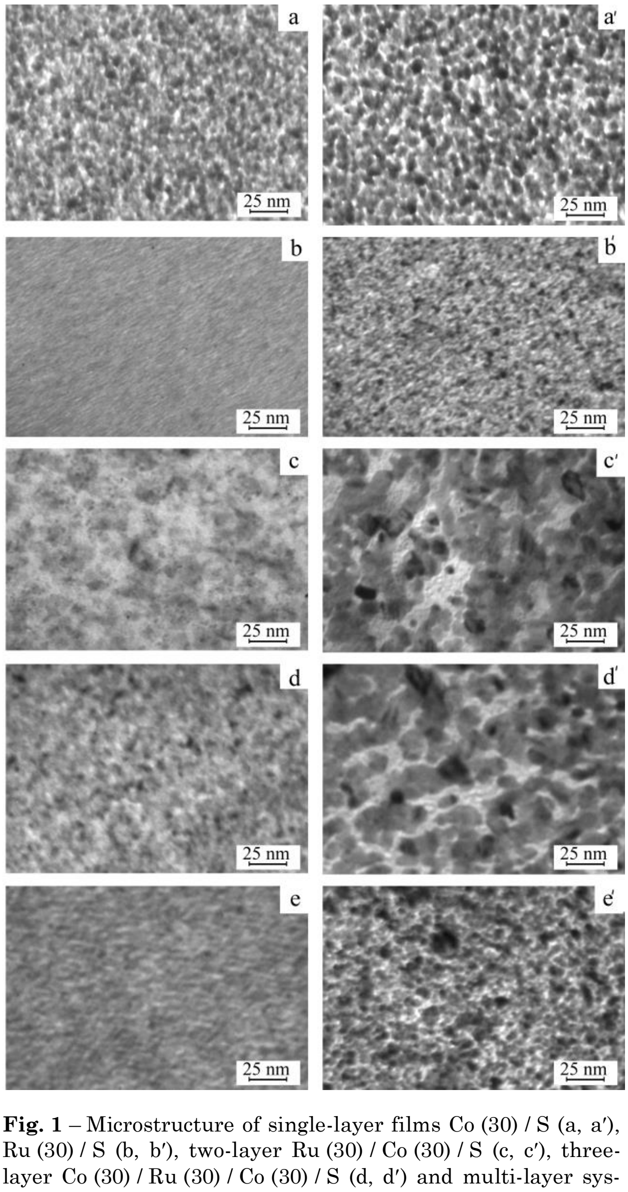

Fig. 1 – Microstructure of single-layer films Co (30) / S (a, a′), Ru (30) / S (b, b′), two-layer Ru (30) / Co (30) / S (c, c′), three-layer Co (30) / Ru (30) / Co (30) / S (d, d′) and multi-layer systems [Ru (2) / Co (2)]$_5$ / S (e, e′) at T_a = 300 K (a, b, c, d, e) and 600 K (a′, b′, c′, d′, e′)

The study results summary of the phase composition and microstructure features of film systems based on Co and Ru is given in Tabl. 1. This film structure whose average grain size matter less than 3÷5 nm nanodisperse called. Such systems approach to quasi-amorphous properties by their properties although they still retain the long-range order of the atoms in the crystal lattice. It is possible to trace the general tendency that, after annealing no longer film systems with nanodisperse structure that are composed of Ru layers thicker than 30 nm and Co layers thicker than 5 nm. Only in the case of a three-layer sample Co (30) / Ru (5) / Co (30) / S nanodispersion of Ru layer cannot be traced.

It should be noted that the nanodispersity of film samples based on Ru layers is due to the influence of impurity carbon atoms, serving as centers of amorphization [13]. These impurities get into the film from the surface of the carbon substrate and the carbon crucible during electron-beam condensing process. But the content of these impurities in a total volume of films is insufficient for the formation of carbides in quantity to fix them on an electronogram. By increasing the thickness of the layers of Ru influence of impurities is reduced. In the case of two- (Fig. 1 c, c′) and three-layer films (Fig. 1 d, d′) in the process of thermal annealing as a result of recrystallization processes, the crystalline structure acquires a labyrinthine form and increases the contrast. The maximum average grain size after annealing is about 16 nm. For comparison, the phase composition and microstructure of the multilayer based on Co and Ru with ultrathin layers before and after annealing were investigated (Fig. 1 e, e′).

Fig. 2 show the decoding of electron diffraction patterns from single-layer Ru (30) / S and two-layer Ru (30) / Co (30) / S films annealed up at T_a = 600 K. A clear electronogram corresponding to hcp-Ru without oxide trace can be obtained at d > 20 nm with annealing to T_a = 600 K (Fig. 2 a). The calculated values of the mean values of the lattice parameters are a = 0.270 ± 0.001 nm and c = 0.430 ± 0.001 nm, which are close to tabular values a_0 = 0.2705 nm and c_0 = 0.4281 nm [14].

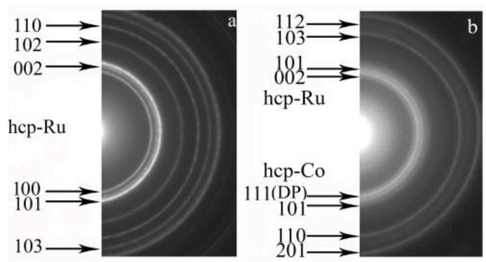

Fig. 2 – Electron diffraction patterns of single-layer Ru (30) / S (a) and two-layer films Ru (30) / Co (30) / S (b) at T_a = 600 K. DP – defect of packing

Two- and three-layer films based on Co and Ru consist of phases hcp-Co + hcp-Ru with lattice parameters close to table. This is most clearly seen in electron diffractions from annealed samples with Ru layer thickness more 30 nm (Fig. 2 b).

On the diffusion profiles presented on Fig. 3 and 4 observed shift the interface between the layers (I). This shift is significant for thicker films (Fig. 4) and is 20÷24 nm. For samples with thinner layers (Fig. 3) such shift is ≈ 5÷12 nm. This interface shift is explained within the concept of Kirkendall effect [15] and the crater effect [16].

Tabl. 1 – Features of microstructure of single-, two- and multilayer systems based on Co and Ru

Film system (nm)	Structural-phase state		Crystallite average size, nm	
	T_a = 300 K	T_a = 900 K	T_a = 300 K	T_a = 600 K
Co (5) / S	Nanodisperse hcp-Co	hcp-Co	2	5
Co (30) / S	hcp-Co + fcc-Co (DP)	hcp-Co + fcc-Co (DP) + fcc-Co	6	8
Co (60) / S			15	20
Ru (5) / S	Nanodisperse hcp-Ru	Nanodisperse hcp-Ru	2	3
Ru (30) / S		hcp-Ru	2	7
Ru (60) / S			2	8
Ru (10) / Co (20) / S	Nanodisperse hcp-Ru + hcp-Co	hcp-Ru+ hcp-Co + fcc-Co (DP)	2	8
Ru (30) / Co (30) / S			3	14
Ru (60) / Co (60) / S			5	16
Co (30) / Ru (5) / Co (30) / S		hcp-Ru+ hcp-Co + fcc-Co (DP)	3	11
Co (30) / Ru (30) / Co (30) / S			3	14
[Ru (2) / Co (2)]$_5$ / S		Nanodisperse hcp-Ru+ hcp-Co	2	4

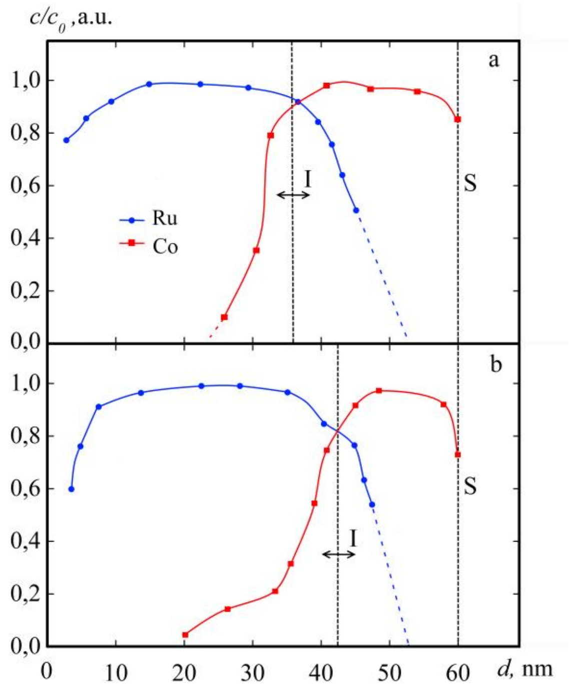

Fig. 3 – Diffusion profiles for Ru (30) / Co (30) / S (a) et T_a, K: 300 (a) and 600 (b)

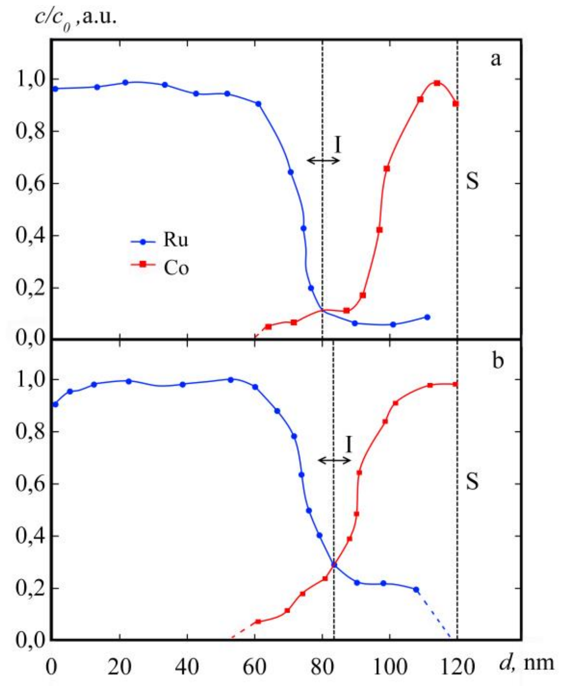

Fig. 4 – Diffusion profiles for Ru (60) / Co (60) / S (a) et T_a, K: 300 (a) and 600 (b)

Diffusion profiles nonannealed samples reflect the contribution the condensation-stimulate diffusion (CSD). In the case annealed samples to 600 K added of contribution of the thermal diffusion (ThD). In all cases ion-stimulate diffusion (ISD) is present, the contribution of which into the total diffusion cannot be taken into account, has a certain effect on a shape of diffusion profiles while using the SIMS technique.

Given the following notation:

$$D_1 = \text{CSD} + \text{ISD},$$
$$D_2 = \text{CSD} + \text{ISD} + \text{ThD},$$
$$D_3 = \text{ThD}$$

and based on the obtained data (Fig. 3, 4), the effective coefficients were calculated using the following relations:

$$l_c = (D_1 \tau_c)^{1/2}, \quad (1)$$

$$l_t = (D_2 \tau_t)^{1/2}, \quad (2)$$

$$l_t - l_c = (D_3 \tau_t)^{1/2}, \quad (3)$$

where l_c and l_t are the diffusion path lengths of atoms for the cases of the CSD + ISD and the ThD, respectively. They were determined as the thickness of scoured lower layer, at which the signal from upperlayer atoms on the SIMS-spectrum vanishes. τ_c and τ_t are the condensation and the thermal annealing times, respectively. Appropriate effective diffusion coefficients for double-layer films Ru / Co / S with relatively thin and thick layers were calculated and are presented in Tabl. 2.

The difference of 2-3 orders received in the effective diffusion coefficients in nonannealed samples related to higher grain-boundary diffusion in films with thicker layers.

Tabl. 2 – Effective diffusion coefficients of atoms in two-layer film systems based on Co and Ru

Diffusion couple	D_1 10^{19}, m^2 / sec.	D_2 10^{19}, m^2 / sec.	D_3 10^{19}, m^2 / sec.
Film system: Ru (30) / Co (30) / S			
Ru → Co	2.1	0.3	0.1
Co → Ru	2.7	4.0	0.8
Film system: Ru (60) / Co (60) / S			
Ru → Co	3.0	4.4	0.1
Co → Ru	1.8	4.5	1.1

4. CONCLUSIONS

The peculiarities of crystal structure and phase composition of two- and three-layer film systems based on Ru and Co in the range of layer thicknesses 5÷60 nm before and after annealing to temperature 600 K. It is shown that the two-layer Co / Ru / S and three-layer film systems Co / Ru / Co / S consist of phases hcp-Co + hcp-Ru. Summary results showed that the film system composed of Ru layers with thickness less than 30 nm have a nanodispersed structure with an average crystallite size less 3÷5 nm. After annealing the average crystallite value is increased to the maximum value 16 nm.

Investigation of diffusion profiles of two-layer film systems Co / Ru / S showed that before and after annealing the individuality of the layers remains.

Based on the results obtained, it can be argued that the best conditions in terms of stability performance characteristics synthetic antiferromagnetic film functional layers based on Ru and Co for metal spin-valves there is a choice of Ru layer thickness 5÷30 nm and the thickness of the Co layers 30 nm and followed annealing up to 600 K.

The work has been performed under the partial financial support of the Ministry of Education and Science of Ukraine (project № 117U003925 (2017-2020)).

Структурно-фазовий стан та дифузійні процеси в плівкових структурах на основі Co і Ru

І.В. Чешко[1], А.М. Логвинов[1], А.І. Салтикова[2], С.І. Проценко[1]

[1] *Сумський державний університет, вул. Римського-Корсакова, 2, 40007 Суми, Україна*
[2] *Сумський державний педагогічний університет ім. А. С. Макаренка, вул. Роменська, 87, 40002 Суми, Україна*

Представлені результати дослідження кристалічної структури, фазового складу та дифузійних процесів у плівкових системах на основі Co та Ru в діапазоні товщин 5÷60 нм до і після відпалювання до температури 600 К. Було показано, що плівкові системи Co / Ru / П та Co / Ru / Co / П складаються з фази ГЩП-Co та ГЩП-Ru. Плівкові системи до складу яких входять шари Ru до і після відпалювання мають нанодисперсну кристалічну структур. Середній розмір кристалітів зразків до відпалювання не перевищує 3÷5 нм, після відпалювання максимальний середній розмір становив 16 нм для зразків з товщиною шарів 60 нм Результати дослідження дифузійних процесів двошарових плівкових систем Co / Ru / П в різних діапазонах товщин показали, що до і після відпалювання зберігається відносна індивідуальність окремих шарів оскільки розраховані значення ефективних коефіцієнтів термічної дифузії для відносно тонких та відносно товстих плівок лежать в межах від 0.1 до 1.1 · 10^{-19} м²/ с.

Ключові слова: Тонка плівка, Синтетичний антиферомагнітний шар, Кристалічна структура, Фазовий склад, Дифузія, Вторинна мас-спектрометрія

REFERENCES

1. A.A. Kamasheva, P.V. Leksina, N.N. Garif'yanova, A.A. Validova, J. Schumannb, V. Kataevb, B. Büchnerbc, I.A. Garifullina, *J. Magn. Magn. Mater.* **459**, No 7 (2018).
2. C.J. Durrant, L.R. Shelford, R.A.J. Valkass, R.J. Hicken, A.I. Figueroa, A.A. Baker, G. van der Laan, L.B. Duffy, P. Shafer, C. Klewe, E. Arenholz, S.A. Cavill, J.R. Childress, J.A. Katine, *Phys. Rev. B* **96**, 144421 (2017).
3. D. Louis, Ia Lytvynenko, T. Hauet, D. Lacour, M. Henh, S. Andrieu, F. Montaigne, *J. Magn. Magn. Mater.* **372**, 233 (2014).
4. R. Matsumoto, H. Arai, S. Yuasa, H. Imamura, *Appl. Phys. Express* **8**, 6 (2015).
5. G.W. Anderson, Y. Huai, M. Pakala, *J. Appl. Phys.* **87**, 5726 (2000).
6. B. Kocamana, N. Akdoğanab, *J. Magn. Magn. Mater.* **456**, 17 (2018).
7. P. Wiśniowski, *J. Appl. Phys.* **100**, 013906 (2006).
8. S. Protsenko, I. Cheshko, L. Odnodvorets, *Tech. Phys. Lett.* **35**, No 10, 903 (2009).
9. S.I. Vorobiov, I.V. Cheshko, A.M. Chornous, I.O. Shpetnyi, *Metallofiz. Nov. Tekhnol.* **35** No 12, 1645 (2013).
10. S.I. Vorobiov, O.V. Shutylieva, I.M. Pazukha, A.M. Chornous, *Tech. Phys.* **59** No 11, 1644 (2014).
11. P.H. Chan, X. Li, P.W.T. Pong, *Vacuum* **140**, 111 (2017).
12. A.G. Kolesnikov, V.S. Plotnikov, E.V. Pustovalov, A.S. Samardak, L.A. Chebotkevich, A.V. Ognev, O.A. Tretiakov, *Sci. Report.* **8**, 15794 (2018).
13. V.K. Portnoi, A.V. Leonov, A.N. Streletskii, A.I. Logacheva, *Phys. Metals Metallogr.* **115** No 3, 277 (2014).
14. H.J. Jung, J.H. Han, E.A. Jung, B.K. Park, J.-H. Hwang, S.U. Son, C.G. Kim, T. Chung, *Chem. Mater.* **26,** 7083 (2014).
15. A. Paul, M.J. Hvan Dal, A.A. Kodentsov, F.J. Jvan Loo, *Acta Mater.* **52** No 3, 6239 (2004).
16. D.S. McPhail, *J. Mater. Sci.* **41** No 3, 873 (2006).